Influence of Field Size, Depth, Nominal Dose Rate and Stem Length on Ion Recombination Correction Factor in Therapeutic Photon Beam

A. I. Abd El-Hafez[1], Hany A. Shousha[*1], M. S. Zaghloul[2] and M. A. Abou Zeid[3]
[1]Radiation Metrology Dept., National Institute for Standards (NIS), Giza, Egypt.
[2] National Cancer Institute (NCI) - Cairo University, Cairo, Egypt.
[3] Faculty of Science - Mansoura University, Al-Mansoura, Egypt.
[*]drshousha@yahoo.com

Abstract: The use of ionization chamber in linear accelerator radiotherapy photon dosimetry requires various corrections to the measured charges, one of these being the ion recombination correction factor (k_s). As stated by the IAEA (2000) TRS-398 dosimetry protocol, k_s was characterized for the available thimble ionization chamber PTW 30006 using two pulsed megavoltage photon beams 6 and 10 MV. The dependence of the k_s values against the changing of field size, water depth, nominal dose rate and stem length was studied. For photon energy 10 MV, k_s shows an increase with the field size and for photon energy 6 MV, k_s values decrease from field size 4x4 cm^2 to 10x10 cm^2 and increase at field sizes larger than 10x10 cm^2. Also, k_s values are inversely proportional with the water depth and directly proportional with the nominal dose rate and stem length, for both photon energies. It is also recommended to determine the absorbed dose at lower (*p.r.f*) pulse repetition frequency or nominal dose rate. If the dose is determined at the highest (*p.r.f*), a correction must be introduced in the assessment of the dose related to the ion recombination correction factor k_s difference at different *p.r.fs*. These measurements help to correct k_s values at different dosimetry conditions and minimize the errors in the assessment of the radiotherapeutic dose calculations.
[A. I. Abd El-Hafez, Hany A. Shousha, M. S. Zaghloul and M. A. AbouZeid. **Influence of Field Size, Depth, Nominal Dose Rate and Stem Length on Ion Recombination Correction Factor in Therapeutic Photon Beam.** Journal of American Science 2011;7(3):206-213]. (ISSN: 1545-1003). http://www.americanscience.org.

Key words: Ion recombination correction factor, ionization chamber, megavoltage x-ray, pulsed photon beams and linear accelerator.

1. Introduction:

In most radiotherapy clinics the dose delivered to a given point in the medium is determined by measuring the amount of charge (Q) produced in a small cavity located at that point in the medium [1, 2]. The cavity is usually an ionization chamber filled with air at ambient temperature and pressure.

The dose delivered to the medium can be calculated from the total charge, or saturation charge, produced in the air cavity according to the Spencer-Attix cavity theory, [3]. The response of a given ionization chamber depends not only on the radiation dose, dose rate and chamber polarity [4] but also on the voltage applied between the measuring and collecting electrodes of the chamber [5, 6, 7]. The charges produced in the chamber by radiation may differ from the charges that are actually collected. These discrepancies (charge losses or excess charges) occur as a result of constraints imposed by the physics of ion transport in the chamber sensitive volume and the chamber electrical design. Charge losses in the chamber are caused by ion recombination; excess charges by charge multiplication and electrical breakdown. Both the charge recombination and charge multiplication are influenced by the potential applied to the ionization chamber. A plot of chamber response, i.e., current (I) or charge (Q) against the applied voltage (V) for a constant dose rate or dose, respectively, is called saturation curve, first rising linearly with voltage at low voltages, then reaching a saturation at high voltages and eventually breaking down at even higher voltages [8, 9]. The ratio Q(V) /Q_{sat} or I(V) / I_{sat} , where (Q_{sat}) and (I_{sat}) are the saturation values of Q and I, respectively, is referred to as the collection efficiency (*f*) of the ionization chamber at the applied voltage (V), (1).

In saturation, all charges produced by radiation are collected and produce directly the (Q_{sat}) and (I_{sat}) for use in dosimetry protocols. When the chamber is used below saturation, some of the charges produced by radiation actually recombine and lead to loss of the dosimetric signal. This charge loss occurs through three different mechanisms:

(1) Initial recombination represents the recombination that occurs between ions produced within the track of a single ionizing particle and is thus independent of dose rate.

For initial recombination, (1/Q) was shown to vary linearly with (1/V), [10, 11].

(2) General recombination, in contrast to initial recombination, applies to ions produced in different ion tracks, which meet and recombine, and thus depends on dose rate. For general recombination, (1/Q) in the near saturation region (f > 0.7) was found to vary linearly with ($1/V^2$) in continuous beams, [10, 12, 13]. In electronegative gases, such as air, it was shown by some authors [10, 11, 14, 15], that in the near saturation region, initial recombination is negligible in comparison with general recombination.

(3) Ionic diffusion loss: charges diffuse against the electric field. For thermal diffusion of ions against the applied chamber potential it was found that (1/Q) also follows a linear relationship with (1/V) in the near saturation region.

For studies of ionic recombination losses, ionizing radiation beams are placed into three categories:

(i) *Continuous radiation* (e.g., cobalt beams and orthovoltage x rays).

(ii) *pulsed beams* (e.g., non-scanned linac x ray beams and electrons).

(iii) *Scanned pulsed beams* (e.g., scanned linac beams).

On the light of the two voltages technique which suggested by Boag and Current [16], describing the ion recombination correction for a small cylindrical ionization chamber exposed to pulsed radiation, [17], proposed an approximation for the ion recombination (P_{ion}) or (k_s) for constructed in the form of quadratic equation and working both pulsed and pulsed swept radiation. This quadratic equation is

(P_{ion}) or (k_s) = (1)

$$a_o + a_1\left(\frac{M_N}{M_L}\right) + a_2\left(\frac{M_N}{M_L}\right)^2$$

Where,

(M_N) is the chamber signal determined at the normal operating voltage (V_N).

(M_L) is the chamber signal determined at a lower voltage (V_L).

(a), (a_1) and (a_2) are constants obtained from standard polynomial fitting program, (18). This equation is adopted by the [19] TRS-398 dosimetry protocol.

2. Material and Methods

The ion recombination correction factor k_s was measured for two pulsed photon radiation beams 6 and 10 MV produced by medical linear accelerator Philips SLi15 which is manufactured in England. A Farmer-type, 0.6 cm^3 vented water proof ionization chamber of model PTW30006, manufactured in Germany, was used in our experiment. The chamber is of rugged construction, since the wall material is graphite with a protective acrylic cover and the collecting electrode is made of aluminum. The readings were taken using an electrometer (Victoreen model 530) , manufactured in U.S.A., connected to the ionization chamber where the normal operating bias voltage V_N adjusted to be at the possible maximum voltage, V_N = +382.5 volts, with positive polarity. The lower operating bias voltage was chosen to be one third of V_N, V_L = +127.5 volts, as recommended by the TRS-398 dosimetry protocol [19].

The amount of irradiation necessary to provide stable readings after decreasing the bias was measured for the chamber by saturating the chamber with 500 monitor units and then reversing the bias. Readings were immediately taken at 50 monitor unit increments until a stable reading was obtained, [20].

A water phantom of model Med-Tec, manufactured in U.S.A., was used in the water measurements and it is constructed from (9.525mm)-thick clear acrylic material of volume 38 x 38 x 38 cm^3 and provided with horizontal scale and manual depth dose apparatus.

For both photon energies 6 and 10 MV, the measurements were performed under the reference conditions where the gantry angle = 0^0, the distance between the radiation focus and water surface FSD = 100 cm, the field size 10x10 cm^2 and the reference water depth = 10 cm, as recommended by the [19] TRS-398 dosimetry protocol, fig. (1).

The variation of k_s was determined against the field size changing at FSD=100 cm where the ionization chamber was located at constant reference water depth equal to 10 cm. Also, the variation of k_s was measured against the water depth changing where the field size kept constant and equal to 10x10 cm^2 at FSD = 100 cm. k_s was determined due to the variation between three available nominal dose rate 100, 300 and 600 M.U./ min.

As a study of the stem effect on k_s, the measurements were done in the air where the distance between the radiation focus and the chamber central axis (FCD) = 100 cm with two build up caps suitable for each photon energy 6 and 10 MV and the field size was equal to 10x35 cm^2 where X-side = 35 cm and Y-side = 10 cm. The zero position is considered when the center of ionization chamber sensitive volume is located at the field center. In the case of the ionization chamber longitudinal central axis was adjusted to be parallel to the X-side, where the stem length was changing and moving away from the field center, the k_s was calculated as:

$$(k_s)^{Par.} = a + a_1((M_N)^{Par.}/(M_L)^{Par.}) + a_2((M_N)^{Par.}(M_L)^{Par.})^2. \quad (2)$$

In the other case, when the chamber longitudinal central axis was oriented in a direction perpendicular to X- side, the stem length was constant and k_s was calculated as:

$$(k_s)^{Per.} = a_o + a_1((M_N)^{Per.}/(M_L)^{Per.}) + a_2((M_N)^{Per.}/(M_L)^{Per.})^2. \quad (3)$$

Where

$(M_N)^{Par}$, $(M_N)^{Per}$ is the electrometer reading (in charge mode) at normal operating voltage V_N = +382.5 volt when the ion chamber longitudinal central axis is parallel and perpendicular to the X-side of the field respectively.

$(M_L)^{Par}$, $(M_L)^{Per}$ is the electrometer reading (in charge mode) at lower voltage V_L = +127.5 volt when the ion chamber longitudinal central axis is parallel and perpendicular to the X-side of the field respectively.

3. Results and Discussion:

Figure (2), representing the drawn data of k_s for both photon energies 6 and 10 MV as (Y) axis versus one side of the square field size as (X) axis and the data was fitted using second polynomial fitting method.

For photon energy 10MV, the value of k_s is increasing with increasing the field size. For photon energy 6MV the value of k_s is decreasing from field size 4x4 cm^2 to 10x10 cm^2, but the value of k_s is increasing when the field size increasing beyond 10x10 cm^2. As the field size is increasing, more portions of the ionization chamber stem and the cable is included in the field and that will affect the collected charges; where some of the ionized charges will be lost in the ionization chamber body and the ion recombination correction factor (k_s) needs to increase to compensate this charges loss. Also, one can observe that the values of k_s for photon energy 10MV is larger than the values of k_s for photon energy 6MV all over the field size increasing range, except at the smallest measured field size 4x4 cm^2, where the values of k_s for both photon energies become very close to each other. That is because at small field sizes the radiation field does not exceed the boundary of the ion collective sensitive volume, so no extra effects can appear from the ion chamber body. So, it is concluded that to increase the accuracy of absorbed dose determination at field sizes differ than 10x10 cm^2, it is recommended to calculate the ion recombination correction factor k_s for each field size and for all available photon energies.

The two curves in figure (3) describe the behavior of k_s for both photon energies 6 and 10 MV, as (Y) axis against water depth as (X) axis. It is obvious from the figure that the values of k_s are decreasing with increasing the water depth for both photon energies 6 and 10 MV. That is because at the small depths near the build up region, the photon beam interacts with the ionization chamber measuring electrode causing a loss of electrons from the measuring electrode which is not fully compensated by arrival electrons from the upper layers of the phantom. Also, it is notable that the values of k_s for photon energy 10MV are higher than the values of k_s for photon energy 6MV all over the increasing range of the water depth. But at the higher water depths, the values of k_s for both photon energies become very close to each other, that is because the dose rate is decreasing with increasing of water depth, which affects the ion recombination of the ionization chamber.

Table (I), shows the variation of k_s against machine nominal dose rate or machine pulse repetition frequency (*p.r.f*) changing with field size = 10x10 cm^2 and water depth = 10 cm at FSD = 100 cm, with constant water temperature and air pressure for each individual measurement at each photon energies 6 and 10 MV.

In the table (I), the values of k_s for both photon energies 6 and 10 MV are increasing with the increasing of the machine nominal dose rate or (*p.r.f*). It is obvious that the variation of k_s values in the 6MV photon beam is smaller than the k_s values for the 10MV photon beam, but at the lowest available nominal dose rate (100 M.U./min.), where the k_s values for both photon energies are close to each other. Since the value of k_s stated by equation (1) is valid if no overlapping of clouds of ions from different beam pulses occurs, [21]. So, at low (*p.r.f*), the duration time of the pulses is bigger than the collection time of the ionization chamber and that makes most of the charges produced by the ionization are well collected for both photon energies. But at higher (*p.r.f*) the pulses duration is decreased a little than the collection time of the ionization chamber, so there will be some sort of overlap between collected charges and some ions will be lost. Also, this phenomenon increases with the increasing of the energy.

Figures (4, (a) and (b)), show the curves of k_s versus the distance of the central measuring volume of the ionization chamber from the field center (distance off axis) in cm, for both photon energies 6 and 10 MV and in the two directions parallel and perpendicular to (X)-side. When the distance off axis is increasing, it means the length of the stem and cable is decreasing.

From figure (4, (a)), it can be noted that the k_s values of the photon energy 6MV are inversely proportional to the distance off axis (i.e. stem length decreases) when the chamber is directed parallel to (X) axis, and directly proportional to distance off axis (i.e. stem length is constant) in the direction perpendicular to (X) axis. The two curves of k_s values of the photon energy 10MV drawn in fig. (4, (b)), are inversely proportional to the distance off axis in a direction parallel (i.e. stem length is decreasing) and perpendicular (i.e. stem length is constant) to the (X) axis. Nevertheless, Bruggmoster et al. [7], stated that there is no influence on radiation type and energy on the recombination correction factor k_s and there is a linear relationship between k_s and the dose per pulse (DPP) up to 5 mGy/pulse. Also, they found that at dose per pulse values above 1 mGy, the method of general equations with coefficients dependent on the chamber type gives more accurate results than the Boag method. This method was already proposed by Burns and McEwen [22] and to avoid comprehensive and time consuming measurements of Jaffé plots which are a prerequisite for the application of the multi-voltage analysis (MVA) or the two voltage analysis (TVA). Many other investigators are concerned with the ion recombination correction factor k_s [5, 6].

Table (I): Ion recombination correction factor (k_s) of the ionization chamber (PTW30006) versus the variation of the nominal dose rate at the reference condition for two photon energies 6 and 10 MV.

Dose Rate in (**M.U./min.**)	Photon energy (**6MV**)		Photon energy (**10MV**)	
	k_s	Standard Deviation	k_s	Standard Deviation
100	1.0008	± 0.00117	1.0020	± 0.00090
300	1.0009	± 0.00041	1.0029	± 0.00040
600	1.0011	± 0.00043	1.0039	± 0.00071

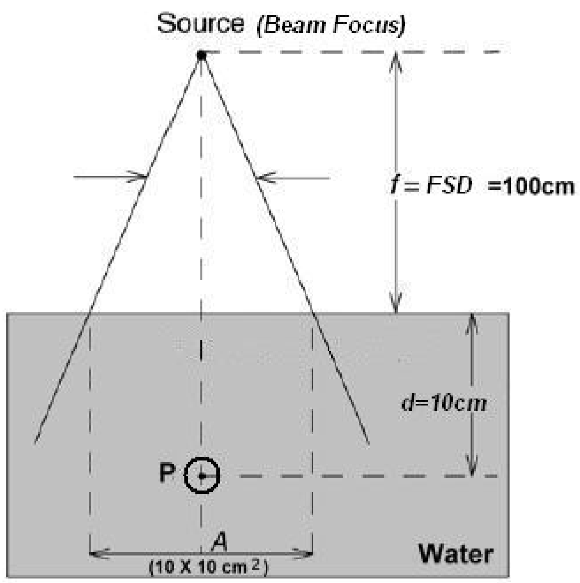

Figure (1): The reference condition of the measurements where field size (A) = 10x10 cm^2 at the distance between the beam focus and water surface (FSD) = 100 cm and the ionization chamber is located at position (P), where the water reference depth (d) = 10 cm.

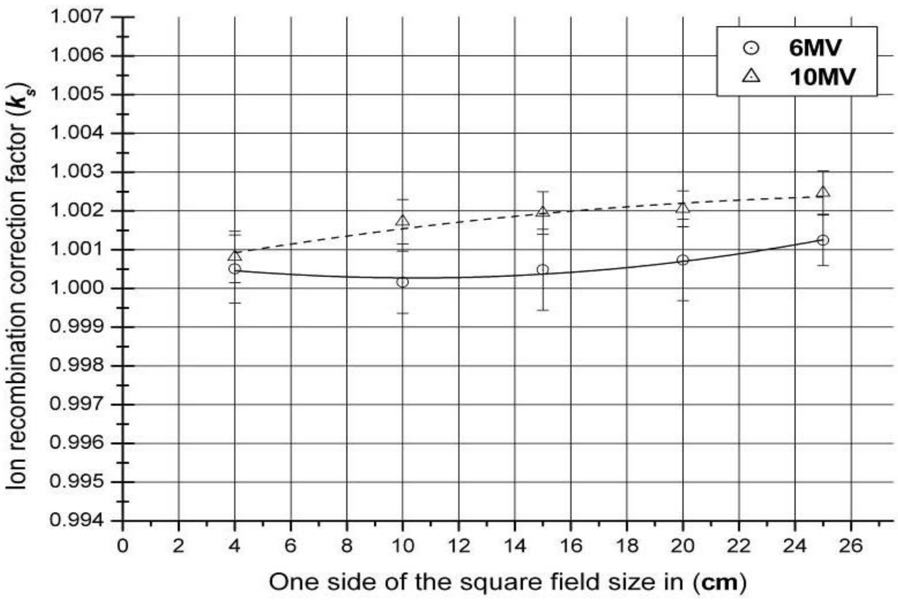

Figure (2): The variation of ion recombination correction factor ks versus the field size at FSD = 100cm and water depth = 10cm for photon energies 6 and 10 MV.

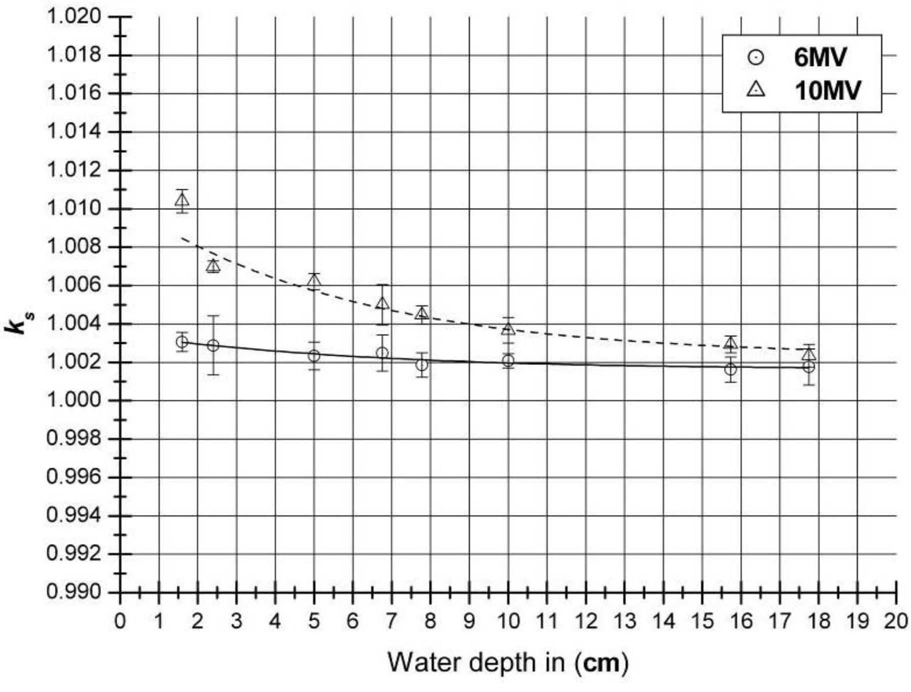

Figure (3): Ion recombination correction factor ks versus the water depth changing of field size=10x10 cm2 at FSD=100cm and for photon energies 6 and 10 MV.

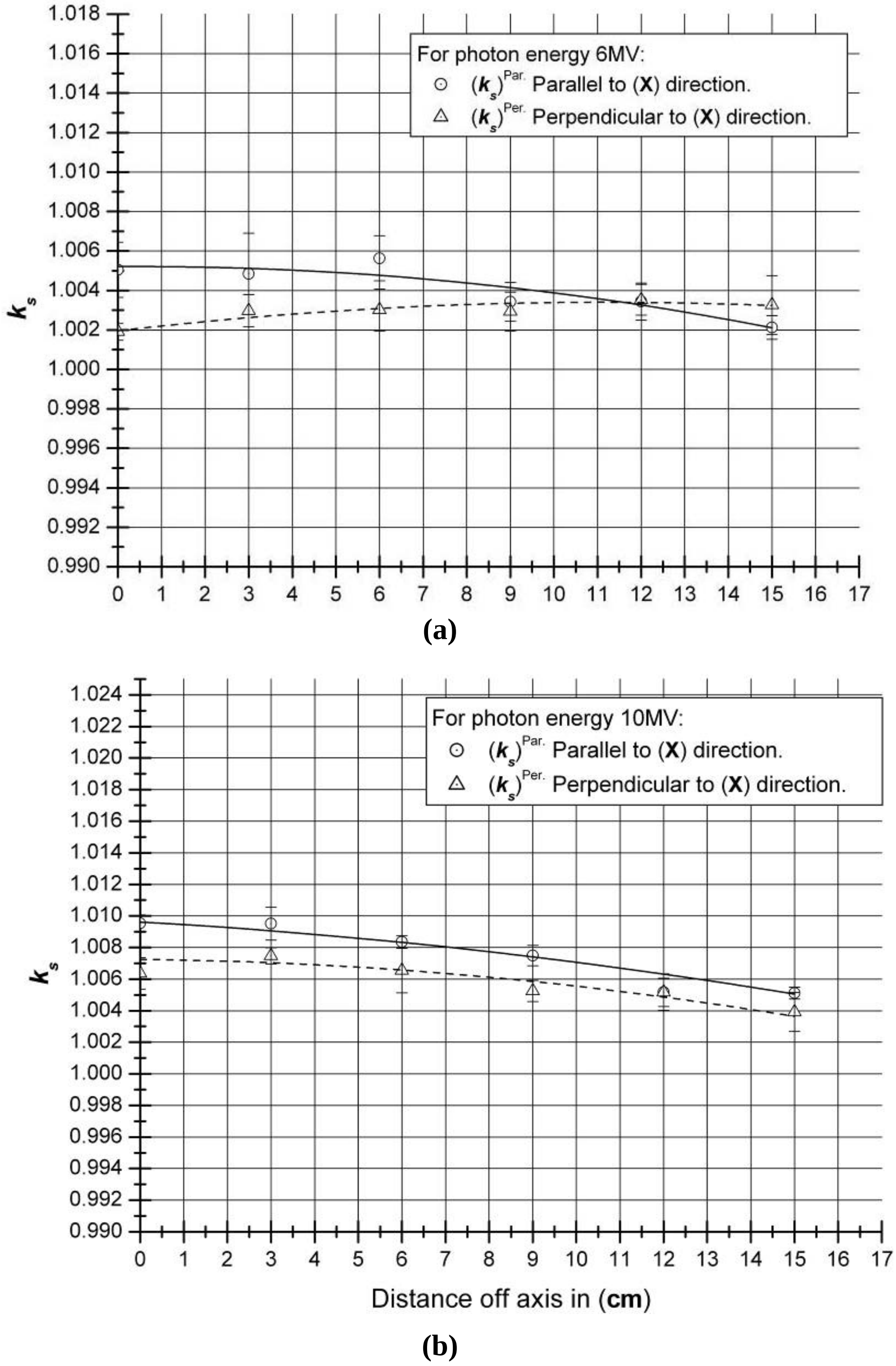

Figure (4) Ion recombination correction factor ks versus the stem length variation in parallel and perpendicular to the (X) axis of the beam plane at FCD = 100cm in the air with suitable build up caps for photon energies: (a) 6MV and (b) 10MV.

4. Conclusions:

To increase the accuracy of the absorbed dose determination at field sizes differ than 10x10 cm^2, using the ionization chamber PTW30006 exposed to pulsed photon beams of energies 6 and 10 MV, it is recommended to measure the ion recombination correction factor (k_s) for each field size. Also, when measuring depth doses, it should account for the change in the ion recombination correction factor (k_s) as a function of depth in phantom. It is better to determine the absorbed dose at low pulse repetition frequency (*p.r.f*) or machine nominal dose rate and if the absorbed dose is determined at the highest (*p.r.f*), a correction must be introduced in the calculation of the dose related to the ion recombination correction factor (k_s) difference at deferent (*p.r.f*s). The amount of the stem length that covered by the radiation field will affect on the ion recombination of the ionization chamber and the value of k_s must be calculated as a function of the stem length.

Corresponding author
Hany A. Shousha
Radiation Metrology Dept., National Institute for Standards (NIS), Giza, Egypt
drshousha@yahoo.com

5. References:

1. Podgorsak, E. B. Review of Radiation Oncology Physics: A handbook for teachers and students, IAEA, Educational Reports Series, Vienna, Austria, (2005).
2. Zhe Chen, Francesco d'Errico, Ravinder Nath. Principles and requirements of external beam dosimetry, Radiat. Meas., (December 2006), Vol. 41, No. 1, 1, pp S2-S21.
3. Spencer, L. V. and Attix, F. H. A theory of cavity ionization, Radiat. Res. (1955), 3, 239-254.
4. Abdel-Hafez A. I., Afifi M. B., Zaghloul M. S. and Abou Zeid M. A. Field Size, Water Depth, Nominal Dose Rate and Stem Length Dependence of Polarity Correction Factor of PTW30006 Ionization Chamber Used in 6 and 10 MV Photon Beams. Egyptian Journal of Biophysics. (January 2007). Vol. 13 No.1 pp 71-81.
5. Nisbet, A.; Thwaites, D. I. Polarity and ion recombination correction factors for ionization chambers employed in electron beam dosimetry. Phys, in Med. and Biol., (1998), 43, 2, 435-443.
6. Di Martino F., Giannelli M., Traino A. C., Lazzeri M. Ion recombination correction for very high dose-per-pulse high-energy electron beams. Med. Phys., (2005), 32,7, 2204-2210.
7. Bruggmoser G Saum R., Schmachtenberg A., Schmid F., Schule E. Determination of the recombination correction factor ks for some specific plane-parallel and cylindrical ionization chambers in pulsed photon and electron beams. Phys. Med. Biol., (2007), 52, 2 ,35-50.
8. Sébastien P. Chabod Impact of space charges on the saturation curves of ionization chambers, Nuclear Instruments and Methods in Physics Research Section A (2009): Accelerators, Spectrometers, Detectors and Associated Equipment, 602, 2, 574-580.
9. Sébastien P. Chabod Charge collection efficiency in ionization chambers operating in the recombination and saturation regimes, Nucl. Instru. and Meth. in Phys. Res. A, (2009), 604, 3, 632-639.
10. Scott, P. B. and Greening, J. R., The determination of saturation currents in free-air ionization chambers by extrapolation methods, Phys. Med. Biol. (1963), 8, 51-57.
11. Boutillon, M., and Niatel, M. T., A study of graphite cavity chamber for absolute exposure measurements of Co-60 gamma rays, Metrologia (1973), 9, 139-146,.
12. Boag, J. W. and Wilson, T., The saturation curve at high ionization intensity, Br. J. Appl. Phys. (1952), 3, 222-229.
13. Greening, J. R., Saturation characteristics of parallel-plate ionization chambers, Phys. Med. Biol. (1964), 9, 143-154.
14. Böhm, J., Saturation corrections for plane parallel ionization chambers, Phys. Med. Biol. (1976), 21, 754-759.
15. Boag, J. W., The Dosimetry of Ionizing Radiation, edited by Kase, K. R., Bjärngard, B. E., and Attix, F. H., (1987), Chapter (3), Vol. (2).
16. Boag, J.W., and Currant, J. Current collection and ionic recombination in small cylindrical ionization chambers exposed to pulsed radiation, Br. J. Appl. Phys. (1980), 53, 471-478.
17. Weinhous, M. S., and Meli, J. A. Determining P_{ion}, the correction factor for recombination losses in an ionization chamber, Med. Phys. (1984), 11, 846-849.
18. Bevington, P. R. Data reduction and error analysis for the physical sciences, McGraw-Hill, New York (1969), chap.8.
19. International Atomic Energy Agency (IAEA), "Absorbed dose determination in external beam radiotherapy: An international code of practice for dosimetry based on standards of absorbed

dose to water", Technical Reports Series, TRS-398, Vienna, Austria, (2000).

20. Deblois, F., Zankowski, C., and Podgorsak, E. B. Saturation current and collection efficiency for ionization chambers in pulsed beams, Med. Phys. (2000), 27, 1146-1155.
21. Derikum, K., and Roos, M. Measurement of saturation correction factors of thimble-type ionization chambers in pulsed photon beams, Phys. Med. Biol. (1993), 38, 755-763,.
22. Burns D. T. and McEwen M. R. Ion recombination corrections for the NACP parallel-plate chamber in a pulsed electron beam. Phys. Med. Biol. (1998), 43, 8, 2033-2045.

2/15/2011